ЯДЕРНА ФІЗИКА
NUCLEAR PHYSICS

УДК 539.164 https://doi.org/10.15407/jnpae2025.02.144

R. Nithya Agnes[1,*], G. M. C. V. Bai[2], S. Selvakumar[3], S. C. Vella Durai[4]

[1] *Department of Physics, St. John's College, Palayamkottai, Tamil Nadu, Affiliated to Manonmaniam Sundaranar University, Tirunelveli, Tamil Nadu, India*
[2] *Department of Physics, Government Arts College, Nagercoil, Tamil Nadu, Affiliated to Manonmaniam Sundaranar University, Tirunelveli, Tamil Nadu India*
[3] *Department of Physics, Department of Science and Humanities, Thamirabharani Engineering College, Thatchanallur, Tirunelveli, Tamil Nadu, India*
[4] *PG and Research Department of Physics, Sri Paramakalayani College, Alwarkurichi, Tenkasi, Tamil Nadu, India*

*Corresponding author: nithya.phy@stjohnscollege.edu.in

A COMPREHENSIVE INVESTIGATION OF ALPHA DECAY FINE STRUCTURE IN ODD-ODD AND ODD-EVEN NUCLEI

We conducted a comprehensive investigation of the alpha decay fine structure in odd-even and odd-odd nuclei with atomic numbers between 95 and 101. Utilizing the cubic plus Yukawa plus exponential model, we considered the combined effects of Coulomb, centrifugal, and Yukawa plus exponential potentials as barriers for interacting fragments, supplemented by a cubic potential in the overlapping region. Our calculations of partial half-lives for alpha transitions to excited states demonstrated notable agreement with experimental data, yielding a standard deviation of 1.7671 for logarithmic half-lives. Furthermore, analysis of the fine structure revealed a linear correlation between the branching ratio and decay width in alpha decay for nuclei such as Americium, Berkelium, Einsteinium, and Mendelevium indicating a direct proportionality between these parameters.

Keywords: alpha decay, fine structure, decay energy, nuclei, Yukawa plus.

1. Introduction

Alpha decay stands out as a pivotal decay pathway for heavy and super heavy nuclei, distinguishing itself among various decay channels like proton radioactivity, cluster decay, beta decay, and spontaneous fission. The significance of systematic studies on alpha decay is underscored by its crucial role in probing fundamental properties of nuclear structure. These studies offer significant insights into fundamental nuclear properties, including charge radii, neutron or proton skins, deformation, incompressibility, isospin asymmetry, and shell effects. The process of alpha decay is fundamentally a quantum tunnelling effect, which was first explained by Gamow and by Condon and Gurney. Generally, alpha decay occurs between the ground states of parent and daughter nuclei. But decay to the various excited states of daughter nuclei is also possible and these results in the decay fine structure. Various theoretical models have been applied to elucidate the fine structure of alpha decay in heavily deformed nuclei [1 - 12]. Notably, K. P. Santhosh et al. have extensively studied alpha decay fine structure across different nuclear categories (even-even, even-odd, odd-even, and odd-odd mass nuclei) using the Coulomb and proximity potential model for deformed nuclei [13, 14].

We extend our previous studies on the fine structure of alpha decay in both even-even and even-odd nuclei [15] to investigate alpha transitions within heavy odd-odd and odd-even nuclei in the range $95 \le Z \le 101$ from the ground state of the parent nucleus to various states of the daughter nucleus. In this new analysis, we incorporate hexacontatetrapole deformation β_6 into the parent nuclei, alongside the quadruple β_2 and hexadecaple β_4 deformations.

The structure of this paper is as follows: Section 2 outlines a brief framework of the cubic plus Yukawa plus exponential model (CYEM). Section 3 presents the results and corresponding discussions. Finally, Section 4 provides a summary.

2. Theoretical framework

The half-life of the parent nucleus decaying via alpha emission is calculated by

$$T_{1/2} = \frac{1.433 \cdot 10^{-21}}{E_v}\left[1+\exp\left(\frac{2}{\hbar}\int_{r_a}^{r_b}\left[2B_r(r)V(r)\right]^{1/2}dr\right)\right]. \quad (1)$$

The nuclear inertial mass coefficient $B_r(r)$, associated with the motion in the fission direction, is defined by

$$B_r(r)-\mu = f(r,r_t)K\left(B_r^{irr}-\mu\right), \quad (2)$$

where $K = 16$, $r_t = a_d + R_d$.

Here, a_d is the semimajor or minor axis of the spheroidal daughter nucleus depending on its prolate or oblate shape.

$$f(r,r_t) = \begin{cases} \left(\dfrac{r_t - r}{r_t - r_i}\right)^4, r \le r_t, \\ 0, r \ge r_t \end{cases} \quad (3)$$

$$B_r^{irr} - \mu = \frac{17}{15}\mu \exp\left\{\frac{-128}{51}\left[\frac{r-r_i}{R_o}\right]\right\}. \quad (4)$$

The alpha emission energy is given by

$$Q = \Delta M - \left(\Delta M_d + \Delta M_p\right) + B_{el}. \quad (5)$$

The ΔM, ΔM_d, and ΔM_p are the mass excess of the parent nucleus, daughter nucleus, and the emitted alpha, respectively, taken from the latest evaluated atomic mass table AME 2020. The impact of electron screening on the nucleus, influenced by surrounding electrons, is determined based on the review conducted by D. Lunney, J. M. Pearson, and C. Thibault [16].

The energy of zero-point vibration is derived from the reference

$$E_v = \frac{\pi\hbar}{2}\frac{\left[2Q/\mu\right]^{1/2}}{\left(C_d + C_e\right)}, \quad \mu = \frac{mA_dA_p}{A}, \quad (6)$$

where m is the nucleon mass; A, A_d, and A_p denote the mass numbers of the parent nucleus, the daughter nucleus, and the emitted proton, respectively, and μ is the reduced mass of the system.

The central radii C_d and C_e of the fragments are provided in accordance with

$$C_i = 1.18A_i^{1/3} - 0.48\left(i = d, p\right). \quad (7)$$

The total interaction potential $V(r)$ in the post-scission region can be expressed as

$$V(r) = V_c(r) + V_n(r) + \frac{l(l+1)\hbar^2}{2\mu r^2} - V_{df}(r) - Q, \quad r \ge r_t, \quad (8)$$

where V_c is the Coulomb potential between a spheroid daughter and spherical emitted proton as in Ref. [17]; V_n is the nuclear interaction energy due to the finite range effects of H. J. Krappe et al. [18]; r is the distance between fragment centres; l is the angular momentum taken away by the emitted proton; V_{df} is the change in nuclear interaction energy due to quadruple deformations in the daughter nuclei as in Ref. [18].

The expression for the Coulomb potential in the scenario of an oblate spheroid daughter nucleus, where the shorter axis is aligned along the fission direction, Pik - Pichak obtained

$$V_C(r) = \frac{3}{2}\frac{Z_dZ_pe^2}{r}\left\{\gamma\left(1+\gamma^2\right)arctan\gamma^{-1} - \gamma^2\right\} \quad (9)$$

and in the case of a prolate spheroid daughter nucleus with a longer axis aligned along the fission direction,

$$V_C(r) = \frac{3}{2}\frac{Z_dZ_pe^2\gamma}{r}\left\{\frac{1-\gamma^2}{2}\ln\frac{\gamma+1}{\gamma-1} + \gamma\right\}, \quad (10)$$

where

$$\gamma = \frac{r}{\left(a_d^2 - b_d^2\right)^{1/2}}. \quad (11)$$

Here, Z_d and Z_p denote the atomic numbers of the daughter nucleus and the emitted proton, respectively. Additionally, a_d and b_d represent the semi-major and semi-minor axes of the spheroidal daughter nucleus, respectively.

For two separated spherical nuclei of equivalent sharp surface radii R_d and R_p the nuclear interaction energy V_n of H. J. Krappe et al. [18] is given by

$$V_n = -D\left[F + \frac{r - r_{12}}{a}\right]\frac{r_{12}}{r}\exp\left[\frac{r_{12}-r}{a}\right], \quad (12)$$

where $r_{12} = R_d + R_p$ is the sum of their equivalent sharp surface radii. The depth constant D is given by

$$D = \frac{4a^3g\left(R_d/a\right)g\left(R_p/a\right)e^{-r_{12}/a}}{r_0^2r_{12}}C_s', \quad (13)$$

where

$$g(X) = Xcoshx - sinhx. \quad (14)$$

For the case of two separated nuclei

$$C_s' = \left[C_s(d)C_s(p)\right]^{1/2}. \quad (15)$$

The constant F is given by

$$F = 4 + \frac{r_{12}}{a} - \frac{f\left(R_d/a\right)}{g\left(R_d/a\right)} - \frac{f\left(R_p/a\right)}{g\left(R_p/a\right)}, \quad (16)$$

where

$$f(x) = X^2sinhx. \quad (17)$$

Also

$$R_i = r_o A_i^{1/3} \quad (i = d, p), \tag{18}$$

$$C_s(i) = a_s\left(1 - K_s I_i^2\right) \tag{19}$$

and $I_i = \dfrac{(N_i - Z_i)}{A_i}$. The constants used are taken from Ref. [8] as follows: r_o = 1.16 fm, a = 0.68 fm, a_s = 21.269461 MeV, K_s = 2.388587 MeV.

H. J. Krappe et al. [18] formulated an expression for the nuclear interaction energy when a spherical nucleus (2) interacts with a deformed nucleus (1) whose nuclear surface is specified by polar coordinates r, θ, and ∅ by the equation

$$R(\theta,\varnothing) = R_0\left[1 + \sum_{n=0}^{\infty}\sum_{m=-n}^{n}\beta_{nm}\mathrm{Y}_{nm}(\theta,\varnothing)\right].$$

Then, the change in the nuclear interaction energy due to the quadruple deformation β_2 of nucleus 1 is given by

$$V_{df} = V_n - \frac{4R_e^3 C_s' A_e' \beta_2}{a r_0^2}\sqrt{5/4\pi}.$$

When considering only the spheroidal deformation β_2, the expression for $R(\theta)$ is given by

$$R(\theta) = R_0\left\{1 + \beta_2\left[5/4\pi\right]^{\frac{1}{2}}\left[(3/2)\cos^2\theta - (1/2)\right]\right\}. \tag{20}$$

Here, R_0 is the sharp radius of the equivalent spherical nucleus.

Incorporating Nilsson's hexadecapole deformation β_4 into the parent deformation, Eq. (20) becomes

$$R(\theta) = R_0\left\{1 - \beta_2\sqrt{5/4\pi}\left[(3/2)\cos^2\theta - 1/2\right] + \beta_4\sqrt{9/4\pi}\,(1/8)\left[35\cos^4\theta - 30\cos^2\theta + 3\right]\right\}. \tag{21}$$

If hexacontatetrapole deformation β_6 is introduced in the parent deformation, Eq. (21) takes the form:

$$R(\theta) = R_0\left[\begin{array}{l} 1 + \beta_2\left(\frac{5}{4\pi}\right)^{1/2}\left(\frac{3}{2}\cos^2\theta - \frac{1}{2}\right) + \beta_4\left(\left(\frac{9}{4\pi}\right)\right)^{1/2}\frac{1}{8}\left(35\cos^4\theta - 30\cos^2\theta + 3\right) + \\ + \beta_6\sqrt{\frac{13}{4\pi}}\left(\frac{1}{16}\left(231\cos^6\theta - 315\cos^4\theta + 105\cos^2\theta - 5\right)\right) \end{array}\right]. \tag{22}$$

The configuration of the potential barrier within the overlapping region which connects the ground state and the contact point, is approximated using a third-order polynomial as proposed by J. R. Nix [19] having the form

$$V(r) = -E_v + \left[V(r_t) + E_v\right] \times$$
$$\times\left\{S_d\left(\frac{r - r_i}{r_t - r_i}\right)^2 - S_p\left(\frac{r - r_i}{r_t - r_i}\right)^3\right\}, \; r_i \le r \le r_t. \tag{23}$$

Here, r_i represents the distance between the centres of mass of two portions of the daughter and the emitted proton within the deformed parent nucleus.

Consider a planar section that divides the parent nucleus into two unequal portions, each with masses corresponding to the heavy and light nuclei involved in the decay. If h_1 and h_2 represent the heights of the heavy and light spherical segments, and R_o is the radius of the parent nucleus, then the distance between the centres of mass is given by

$$r_i = \frac{3}{4}\left[\frac{h_1^2}{R_o + h_1} + \frac{h_2^2}{R_o + h_2}\right]. \tag{24}$$

The constants S_d and S_p in Eq. (23) are determined by ensuring the continuity of the potential and its first derivative at the contact point $r = r_t$.

3. Results and discussion

Using the CYEM, we thoroughly examined the fine structure of alpha decay for each transition of odd-odd and odd-even nuclei in the range $95 \le Z \le 101$ by incorporating spin-parity effects and a rotational energy term, along with consideration of higher-order deformation parameters. Our calculations depend on input data encompassing the Q-value of alpha decay, as well as the quadrupole β_2, hexadecapole β_4, and hexacontatetrapole β_6 deformation values for parent nuclei and quadrupole β_2, deformation value for daughter nuclei. Furthermore, we take into account the angular momentum transferred by the alpha particle during the decay process. The Q-values for alpha decay were calculated using up-to-date atomic mass data [20], while deformation values were obtained from [21].

The results of our study are presented in Tables 1 and 2. In the provided Tables, the experimental partial half-lives for various excited states of the daughter nuclei have been found using both the experimental total half-life and the alpha decay intensity to the corresponding states, as referenced in [22]. The first column in these Tables indicates the transitions between the initial and final states of the nuclei. States with undefined spin-parity values are enclosed in brackets, and those for which spin-parity

is unknown are denoted by a question mark. In our calculations, these states are treated as favoured transitions. An examination of Tables 1 and 2 shows that the majority of the calculated logarithmic half-life values closely match the experimental data. Our study reveals that a longer decay in half-life signifies stability in the parent nucleus, while a shorter half-life means the daughter nucleus is more stable.

Table 1. **Comparison of calculated and experimental alpha decay half-lives in odd-even nuclei**

Alpha transitions	ℓ_{min}, $h/2\pi$	Q, MeV	$Log_{10}T_{1/2}$, s		$B_{cal.}$, %	Decay width Γ, MeV
			CYEM	Expt. 18]		
$^{241}Am \rightarrow ^{237}Np+\alpha$						
$5/2^- \rightarrow 5/2^+$	1	5.682	10.123	10.136	36.2625	$3.4368\cdot10^{-32}$
$5/2^- \rightarrow 7/2^+$	1	5.648	10.319	10.352	23.0912	$2.1885\cdot10^{-32}$
$5/2^- \rightarrow 5/2^-$	0	5.623	10.391	7.776	19.5635	$1.8542\cdot10^{-32}$
$5/2^- \rightarrow 9/2^+$	3	5.606	10.909	11.403	5.9353	$5.6254\cdot10^{-33}$
$5/2^- \rightarrow 7/2^-$	2	5.579	10.865	8.587	6.5682	$6.2252\cdot10^{-33}$
$5/2^- \rightarrow 11/2^+$	3	5.552	11.228	11.704	2.8474	$2.\ 6987\cdot10^{-33}$
$5/2^- \rightarrow 9/2^-$	2	5.524	11.193	9.484	3.0864	$2.9252\cdot10^{-33}$
$5/2^- \rightarrow 11/2^-$	4	5.456	12.059	11.528	0.4202	$3.9825\cdot10^{-34}$
$5/2^- \rightarrow 3/2^-$	2	5.414	11.862	13.005	0.6614	$6.2684\cdot10^{-34}$
$5/2^- \rightarrow 13/2^-$	4	5.377	12.546	12.324	0.1369	$1.2976\cdot10^{-34}$
$5/2^- \rightarrow (7/2^-)$	2	5.358	12.212	12.591	0.2954	$2.7999\cdot10^{-34}$
$5/2^- \rightarrow 1/2^+$	3	5.350	12.464	14.70	0.1654	$1.5673\cdot10^{-34}$
$5/2^- \rightarrow (5/2^-)$	0	5.322	12.225	12.926	0.2867	$2.7174\cdot10^{-34}$
$5/2^- \rightarrow 5/2^+$	1	5.313	12.355	12.75	0.2125	$2.0144\cdot10^{-34}$
$5/2^- \rightarrow 3/2^+$	1	5.311	12.368	13.227	0.2063	$1.9550\cdot10^{-34}$
$5/2^- \rightarrow 15/2^-$	6	5.286	13.739	12.859	0.0088	$8.3206\cdot10^{-36}$
$5/2^- \rightarrow ?$	1	5.264	12.669	13.199	0.1031	$9.7758\cdot10^{-35}$
$5/2^- \rightarrow (11/2^-)$	4	5.248	13.367	13.102	0.0207	$1.9596\cdot10^{-35}$
$5/2^- \rightarrow 9/2^+$	3	5.230	13.232	13.102	0.0282	$2.6740\cdot10^{-35}$
$5/2^- \rightarrow 7/2^+$	1	5.222	12.942	13.102	0.0550	$5.2138\cdot10^{-35}$
$5/2^- \rightarrow (9/2^-)$	2	5.196	13.254	13.558	0.0268	$2.5419\cdot10^{-35}$
$5/2^- \rightarrow (5/2^-)$	0	5.136	13.440	12.859	0.0175	$1.6564\cdot10^{-35}$
$5/2^- \rightarrow 5/2^-$	0	4.960	14.653	12.860	0.0011	$1.0143\cdot10^{-36}$
$5/2^- \rightarrow 7/2^-$	2	4.926	15.107	13.770	0.0004	$3.5657\cdot10^{-37}$
$5/2^- \rightarrow 9/2^-$	2	4.882	15.424	15.005	0.0002	$1.7185\cdot10^{-37}$
$5/2^- \rightarrow 5/2^+$	1	5.484	11.356	11.366	43.4950	$2.0098\cdot10^{-33}$
$5/2^- \rightarrow 7/2^+$	1	5.452	11.552	11.463	27.6974	$1.2798\cdot10^{-33}$
$5/2^- \rightarrow 5/2^-$	0	5.409	11.739	8.808	18.0069	$8.3206\cdot10^{-34}$
$5/2^- \rightarrow 7/2^-$	2	5.366	12.235	9.688	5.7470	$2.656\cdot10^{-34}$
$5/2^- \rightarrow 9/2^-$	2	5.311	12.583	10.606	2.5789	$1.1917\cdot10^{-34}$
$5/2^- \rightarrow (11/2^-)$	4	5.243	13.500	12.843	0.3122	$1.4426\cdot10^{-35}$
$5/2^- \rightarrow (5/2^+)$	1	5.217	13.041	13.006	0.8983	$4.1510\cdot10^{-35}$
$5/2^- \rightarrow (13/2^-)$	4	5.167	13.999	13.57	0.0990	$4.5725\cdot10^{-36}$
$5/2^- \rightarrow (5/2^-)$	0	5.159	13.347	13.446	0.4441	$2.0519\cdot10^{-35}$
$5/2^- \rightarrow (5/2^+, 7/2^+)$	1	5.137	13.572	13.843	0.2645	$1.2222\cdot10^{-35}$
$5/2^- \rightarrow (9/2^+)$	1	5.125	13.652	13.843	0.2200	$1.0166\cdot10^{-35}$
$5/2^- \rightarrow ?$	0	5.073	13.928	13.215	0.1165	$5.3846\cdot10^{-36}$
$5/2^- \rightarrow ?$	0	5.057	14.038	14.492	0.0905	$4.1798\cdot10^{-36}$
$5/2^- \rightarrow (11/2^+)$	3	5.046	14.551	14.818	0.0278	$1.2828\cdot10^{-36}$
$5/2^- \rightarrow (5/2^-)$	0	4.822	15.714	13.517	0.0019	$8.8136\cdot10^{-38}$

Continuation of Table 1

Alpha transitions	ℓ_{min}, h/2π	Q, MeV	$Log_{10}T_{1/2}$, s		$B_{cal.}$, %	Decay width Γ, MeV
			CYEM	Expt. 18]		
$^{243}Bk \rightarrow ^{239}Am + \alpha$						
$(3/2^-)\rightarrow(5/2^-)$	2	6.921	5.127	4.210	41.6756	$3.4053\cdot10^{-27}$
$(3/2^-)\rightarrow(7/2^-)$	2	6.880	5.305	4.297	27.6619	$2.2602\cdot10^{-27}$
$(3/2^-)\rightarrow(9/2^-)$	2	6.827	5.538	5.316	16.1764	$1.3218\cdot10^{-27}$
$(3/2^-)\rightarrow(11/2^-)$	4	6.765	6.295	5.554	2.8306	$2.3129\cdot10^{-28}$
$(3/2^-)\rightarrow(5/2^+)$	1	6.734	5.804	3.991	8.7676	$7.164\cdot10^{-28}$
$(3/2^-)\rightarrow(7/2^+)$	5	6.701	6.893	4.109	0.7143	$5.8365\cdot10^{-29}$
$(3/2^-)\rightarrow(9/2^+)$	3	6.661	6.500	4.554	1.7656	$1.4426\cdot10^{-28}$
$(3/2^-)\rightarrow11/2^+)$	7	6.604	8.049	5.530	0.0499	$4.0753\cdot10^{-30}$
$(3/2^-)\rightarrow13/2^+)$	5	6.551	7.5860	6.094	0.1448	$1.1835\cdot10^{-29}$
$(3/2^-)\rightarrow(3/2^-)$	0	6.364	7.476	4.262	0.1866	$1.5246\cdot10^{-29}$
$(3/2^-)\rightarrow(5/2^-)$	2	6.335	8.321	4.800	0.0267	$2.1785\cdot10^{-30}$
$^{247}Bk \rightarrow ^{243}Am + \alpha$						
$3/2^-\rightarrow5/2^-$	2	5.936	9.980	10.639	41.4291	$4.777\cdot10^{-32}$
$3/2^-\rightarrow7/2^-$	2	5.894	10.213	10.747	24.2273	$2.7935\cdot10^{-32}$
$3/2^-\rightarrow5/2^+$	1	5.852	10.292	10.150	20.1979	$2.3289\cdot10^{-32}$
$3/2^-\rightarrow7/2^+$	3	5.828	10.804	10.266	6.2131	$7.164\cdot10^{-33}$
$3/2^-\rightarrow (9/2^+)$	3	5.793	11.003	10.640	3.9292	$4.5306\cdot10^{-33}$
$3/2^-\rightarrow(11/2^+)$	5	5.748	11.860	11.778	0.5461	$6.2973\cdot10^{-34}$
$3/2^-\rightarrow3/2^-$	0	5.671	11.254	9.727	2.2045	$2.5419\cdot10^{-33}$
$3/2^-\rightarrow(5/2^-)$	2	5.638	11.684	10.535	0.8190	$9.4440\cdot10^{-34}$
$3/2^-\rightarrow(7/2^-)$	2	5.592	11.960	11.204	0.4338	$5.0021\cdot10^{-34}$
$^{245}Es \rightarrow ^{241}Bk + \alpha$						
$3/2^-\rightarrow(7/2^+)$	1	7.963	1.752	1.820	46.6156	$8.0752\cdot10^{-24}$
$3/2^-\rightarrow(3/2^-)$	0	7.912	1.854	0.615	36.8579	$6.3849\cdot10^{-24}$
$3/2^-\rightarrow(5/2^-)$	4	7.881	2.699	1.405	5.2666	$9.1234\cdot10^{-25}$
$3/2^-\rightarrow(7/2^-)$	2	7.835	2.369	2.042	11.2598	$1.9505\cdot10^{-24}$
$^{247}Es \rightarrow ^{243}Bk + \alpha$						
$7/2^+\rightarrow(7/2^+)$	0	7.511	3.397	2.436	67.3278	$1.8288\cdot10^{-25}$
$7/2^+\rightarrow(9/2^+)$	2	7.444	3.903	3.291	20.9989	$5.7037\cdot10^{-26}$
$7/2^+\rightarrow(11/2^+)$	2	7.380	4.158	4.068	11.6733	$3.1707\cdot10^{-26}$
$^{251}Es \rightarrow ^{247}Bk + \alpha$						
$3/2^-\rightarrow3/2^-$	0	6.645	7.212	5.075	43.7314	$2.7999\cdot10^{-29}$
$3/2^-\rightarrow(5/2^-)$	2	6.613	7.620	6.016	17.092	$1.0944\cdot10^{-29}$
$3/2^-\rightarrow7/2^+$	1	6.603	7.498	6.457	22.6357	$1.4493\cdot10^{-29}$
$3/2^-\rightarrow(7/2^-)$	2	6.573	7.811	6.511	11.0101	$7.0495\cdot10^{-30}$
$3/2^-\rightarrow(9/2^+)$	3	6.561	8.110	6.457	5.5309	$3.5412\cdot10^{-30}$
$^{255}Es \rightarrow ^{251}Bk + \alpha$						
$(7/2^+)\rightarrow (7/2^+)$	0	6.449	8.171	5.691	36.1422	$3.0772\cdot10^{-30}$
$(7/2^+)\rightarrow(9/2^+)$	2	6.412	8.617	6.644	12.9424	$1.1019\cdot10^{-30}$
$(7/2^+)\rightarrow11/2^+)$	2	6.361	8.874	7.235	7.1617	$6.0976\cdot10^{-31}$
$^{255}Md \rightarrow ^{251}Es + \alpha$						
$(7/2^-)\rightarrow5/2^-$	2	7.923	3.074	3.268	27.4185	$3.8473\cdot10^{-25}$
$(7/2^-)\rightarrow7/2^-$	0	7.879	2.967	3.268	35.0788	$4.9222\cdot10^{-25}$
$(7/2^-)\rightarrow7/2^-$	0	7.494	4.454	1.299	1.1430	$1.6038\cdot10^{-26}$
$(7/2^-)\rightarrow(9/2^-)$	2	7.442	4.931	2.569	0.3811	$5.3476\cdot10^{-27}$
$^{257}Md \rightarrow ^{253}Es + \alpha$						
$(7/2^-)\rightarrow7/2^+$	1	7.607	4.125	4.298	37.6621	$3.4210\cdot10^{-26}$
$(7/2^-)\rightarrow(9/2^+)$	1	7.560	4.311	4.429	24.5417	$2.2292\cdot10^{-26}$
$(7/2^-)\rightarrow11/2^+)$	3	7.527	4.880	4.855	6.6201	$6.0139\cdot10^{-27}$
$(7/2^-)\rightarrow$?	0	7.501	4.453	4.730	17.6972	$1.6075\cdot10^{-26}$
$(7/2^-)\rightarrow(5/2^-)$	2	7.468	4.859	4.451	6.9487	$6.3118\cdot10^{-27}$
$(7/2^-)\rightarrow(7/2^-)$	2	7.426	5.029	4.554	4.6979	$4.2673\cdot10^{-27}$
$(7/2^-)\rightarrow(7/2^-)$	0	7.236	5.547	1.885	1.4253	$1.2947\cdot10^{-27}$
$(7/2^-)\rightarrow(9/2^-)$	0	7.172	5.820	3.340	0.4064	$3.6911\cdot10^{-28}$

Table 2. **Comparison of calculated and experimental alpha decay half-lives in odd-odd nuclei**

Alpha transitions	ℓ_{min}, $h/2\pi$	Q, MeV	$Log_{10}T_{1/2}$, s		$B_{cal.}$, %	Decay width Γ, MeV
			CYEM	Expt. [18]		
$^{240}Am \rightarrow ^{236}Np+\alpha$						
$(3^-)\rightarrow(3^-)$	0	5.509	11.008	9.045	5.8079	$4.4787\cdot10^{-33}$
$(3^-)\rightarrow(4^-)$	2	5.467	11.469	9.904	2.0092	$1.5494\cdot10^{-33}$
$(3^-)\rightarrow(5^-)$	2	5.416	11.782	10.90	0.9773	$7.5363\cdot10^{-34}$
$^{244}Bk \rightarrow ^{240}Am+\alpha1$						
$(4^-)\rightarrow(3^-)$	2	6.825	5.543	4.195	47.7565	$1.3066\cdot10^{-27}$
$(4^-)\rightarrow(4^-)$	0	6.782	5.504	4.195	52.2435	$1.4294\cdot10^{-27}$
$^{254}Es \rightarrow ^{250}Bk+\alpha$						
$2^+\rightarrow2^-$	1	6.665	7.234	5.151	41.2211	$2.6617\cdot10^{-29}$
$2^+\rightarrow(4^+)$	2	6.630	7.574	4.988	18.8417	$1.2166\cdot10^{-29}$
$2^+\rightarrow(5^+)$	2	6.588	7.774	5.656	11.8883	$7.6764\cdot10^{-30}$
$2^+\rightarrow(2^-)$	3	6.540	8.254	12.850	3.9366	$2.5419\cdot10^{-30}$
$2^+\rightarrow(6^+)$	2	6.535	8.030	5.961	6.5935	$4.2575\cdot10^{-30}$
$2^+\rightarrow(5^-)$	3	6.528	8.312	6.678	3.4444	$2.2241\cdot10^{-30}$
$2^+\rightarrow(1^+)$	2	6.490	8.249	5.494	3.9821	$2.5713\cdot10^{-30}$
$2^+\rightarrow2^+$	0	6.453	8.169	3.878	4.7876	$3.0914\cdot10^{-30}$
$2^+\rightarrow(3^+)$	2	6.428	8.556	4.833	1.9639	$1.2681\cdot10^{-30}$
$2^+\rightarrow(4^+)$	2	6.395	8.721	5.413	1.3431	$8.6727\cdot10^{-31}$
$2^+\rightarrow?$	0	6.367	8.599	6.070	1.7788	$1.1486\cdot10^{-30}$
$2^+\rightarrow(5^+)$	4	6.349	9.509	6.550	0.2188	$1.4130\cdot10^{-31}$
$^{256}Md \rightarrow ^{252}Es+\alpha$						
$(1^-)\rightarrow(5^-)$	4	7.795	4.183	3.667	15.1222	$2.9933\cdot10^{-26}$
$(1^-)\rightarrow?$	0	7.760	3.456	3.747	80.6523	$1.5965\cdot10^{-25}$
$(1^-)\rightarrow?$	0	7.359	5.047	3.667	2.0683	$4.0941\cdot10^{-27}$
$(1^-)\rightarrow(1^-)$	0	7.319	5.213	2.222	1.4113	$2.7935\cdot10^{-27}$
$(1^-)\rightarrow?$	0	7.253	5.490	2.728	0.7458	$1.4762\cdot10^{-27}$
$^{258}Md \rightarrow ^{254}Es+\alpha$						
$(8^-)\rightarrow(7^+)$	1	7.321	5.261	6.648	58.1838	$2.5012\cdot10^{-27}$
$(8^-)\rightarrow(8^+)$	1	7.241	5.597	6.648	26.8412	$1.1539\cdot10^{-27}$
$(8^-)\rightarrow(9^+)$	1	7.150	5.986	6.648	10.9598	$4.7115\cdot10^{-28}$
$(8^-)\rightarrow(8^+)$	1	6.944	6.897	4.954	1.3452	$5.7830\cdot10^{-29}$
$(8^-)\rightarrow(7^-)$	0	6.917	6.928	4.631	1.2526	$5.3846\cdot10^{-29}$
$(8^-)\rightarrow(8^-)$	0	6.873	7.130	4.131	0.7867	$3.3819\cdot10^{-29}$
$(8^-)\rightarrow?$	0	6.852	7.226	5.117	0.6307	$2.7111\cdot10^{-29}$

These findings are graphically depicted in Figs. 1 and 2. In even-even nuclei, the alpha particle experiences a transition from the ground state of the parent nucleus to the ground state of the daughter nucleus, leading to zero angular momentum. In contrast, in even-odd, odd-odd, or odd-even nuclei, the angular momentum may not be zero. Our calculations specifically account for the minimum angular momentum values in these scenarios. These values of natural angular momentum are determined by applying the conventional law of nuclear spin and parity, expressed as

$$\left|J_i - J_j\right| \le l_a \le \left|J_i + J_j\right| \text{ and } \frac{\pi_i}{\pi_j} = (-1)^{l_a}.$$

In this context, J_i and π_i represent the spin and parity values of the parent nucleus, while J_j and π_j denote the spin and parity values of the daughter nucleus. A parity selection rule determines the permissibility of transitions by conserving parity. If the initial and final states have the same parity, the angular momentum quantum number l_a must be even. Conversely, when the parities differ, l_a must be odd.

The branching ratio for alpha decay to each state of the daughter nucleus is expressed in terms of the partial width of alpha decay $\Gamma(Q_i, l_i)$ as

$$B_i = \frac{\Gamma(Q_i, l_i)}{\sum_n \Gamma(Q_n, l_n)} \cdot 100\,\%.$$

Here, the summation over n includes all states that can be populated during the alpha transition from the ground state of the parent nucleus. The alpha decay of even-even nuclei mainly populates from 0^+ ground state to 0^+ ground state, belonging to

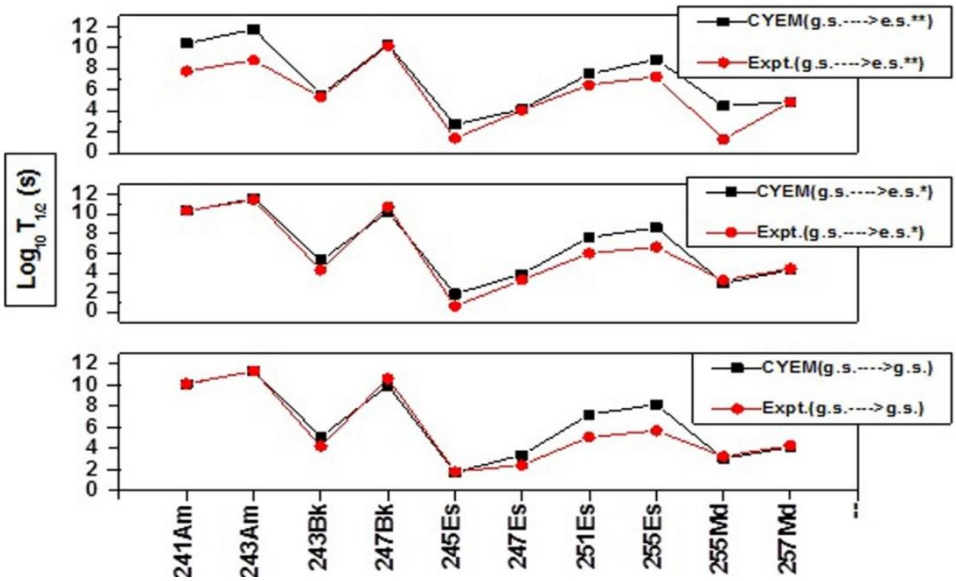

Fig. 1. Comparison of calculated half-lives of odd-even nuclei with the corresponding experimental values (g.s., e.s.* & e.s.** representing the ground state, the first and second excited states, respectively). (See color Figure on the journal website.)

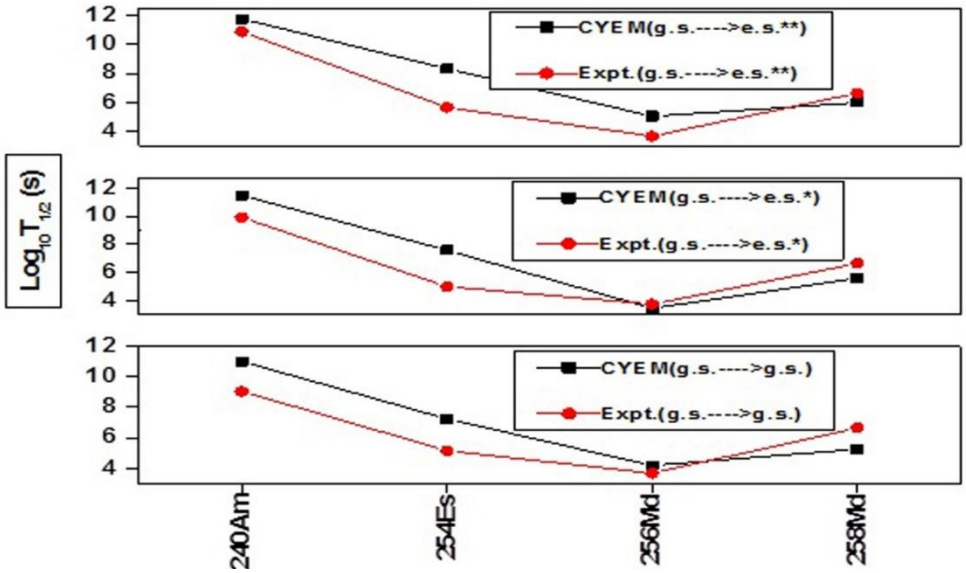

Fig. 2. Comparison of calculated half-lives of odd-odd nuclei with the corresponding experimental values (g.s., e.s.* & e.s.** representing the ground state, the first and the second excited states, respectively). (See color Figure on the journal website.)

favoured alpha transition and the intensity is decreased when the transition proceeds to higher-lying excited states. The situation for odd-mass nuclei is much more complicated, because of the last unpaired nucleons. We calculated the branching ratios for alpha decay to various excited states. In certain decay processes, it was found that the intensity of the alpha decay in the excited state exceeds that in the ground state. This occurrence could be attributed to the unique configuration of excited states, where specific rotational modes may be more pronounced. Additionally, resonant enhancement might take place when the energy of the emitted alpha particle aligns with a resonance in the excited state. Our findings are closely aligned with those of other researchers [23 - 25].

We also calculated the decay width Γ, and tabulated it in Tables 1 and 2. A larger decay width indicates a higher decay rate and a broader energy distribution of the emitted alpha particles. This often correlates with a higher branching ratio for the corresponding decay channel, as the channel becomes more prominent relative to others.

In odd-odd and odd-even nuclei, which have complex nuclear structures, an increased decay width typically reflects more significant energy states or more accessible decay paths, making those channels more probable. From the Tables, we infer that a larger decay width in one of these fine-structure channels implies that the state associated with this channel is relatively short-lived or more accessible, thereby increasing its branching ratio.

The graphs plotting the branching ratio versus the decay width for Americium (Am), Berkelium (Bk), Einsteinium (Es), and Mendelevium (Md) produce straight lines, as shown in Figs. 3 and 4. This indicates a general trend where a larger decay width leads to a higher branching ratio for a given decay channel, reflecting a more accessible or significant decay path.

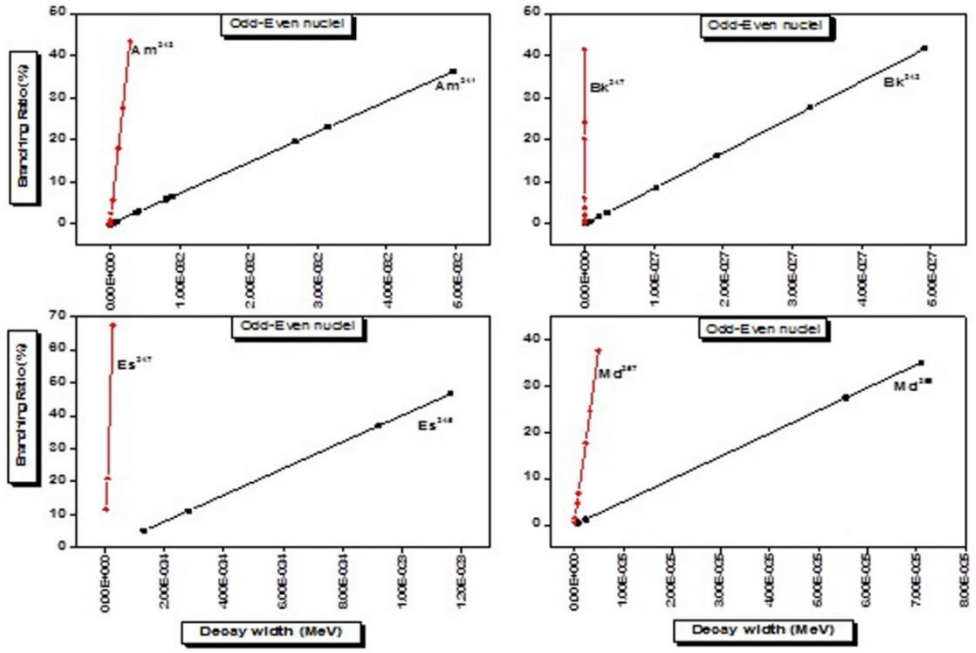

Fig. 3. Graph plotting the branching ratio versus the decay width for the odd-even nuclei of Am, Bk, Es, and Md. (See color Figure on the journal website.)

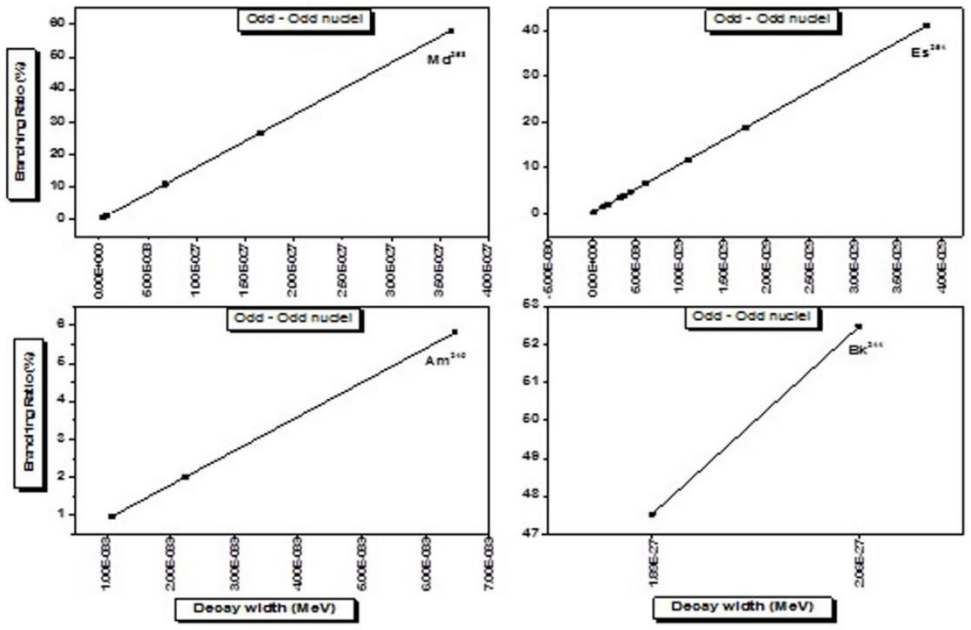

Fig. 4. Graph plotting the branching ratio versus the decay width for the odd-odd nuclei of Am, Bk, Es, and Md.

The hindrance factor (HF) is a quantity used to compare different alpha decay channels, such as decay to the ground state versus decay to excited states. It provides insight into how much a decay process is slowed down due to structural effects like differences in spin, parity, or nuclear configuration. HF is defined as the ratio of reduced widths. It is calculated using the following formula and is illustrated in Fig. 5.

$$HF = \frac{\Gamma_{gs} / P_{gs}}{\Gamma_{ex} / P_{ex}},$$

where Γ is the partial decay width and P is the penetrability of the Coulomb barrier.

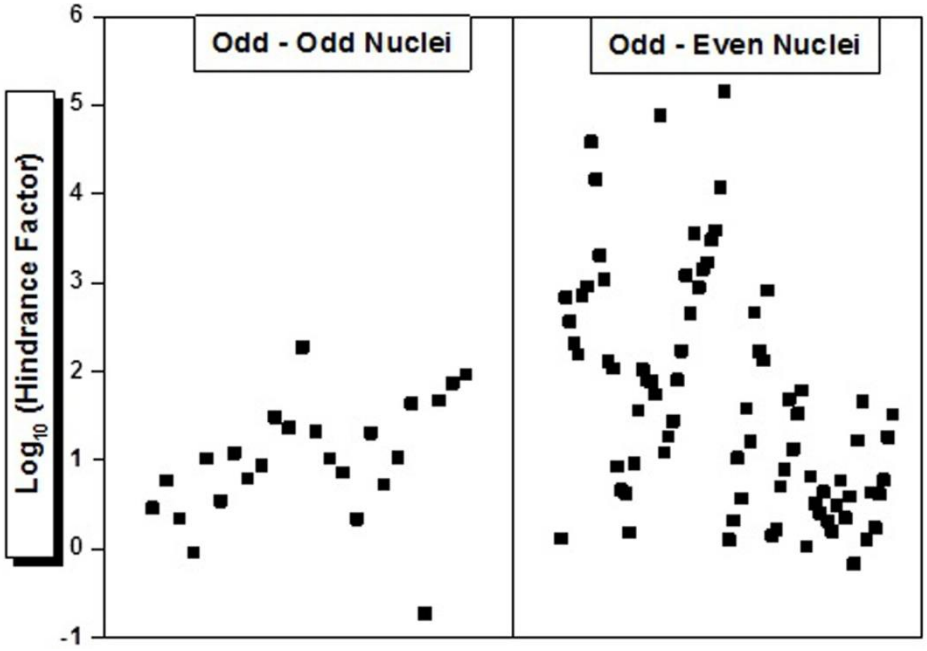

Fig. 5. Computed log HF values for all transitions.

In this study, we analyzed alpha decay transitions in odd-even and odd-odd nuclei by evaluating the logarithmic hindrance factors (log HF), representing the degree of hindrance experienced by the alpha particle during its emission. The calculated average values are as follows:

Odd-even nuclei: log HF = 1.866,
Odd-odd nuclei: log HF = 0.961.

These results indicate that alpha transitions in odd-even nuclei are, on average, more hindered than those in odd-odd nuclei. The higher hindrance in odd-even nuclei can be attributed to pairing effects and less favorable angular momentum matching between the initial and final nuclear states. Conversely, the lower hindrance observed in odd-odd nuclei suggests that alpha transitions are more energetically or structurally favored, potentially due to better spin-parity compatibility [26, 27].

This observation aligns with the understanding that nuclear structure, particularly the arrangement and pairing of protons and neutrons, is crucial in determining the alpha decay probability. However, the relatively low hindrance in odd-odd systems, which are usually expected to be more complex due to unpaired nucleons, may also reflect specific nuclear configurations or transition selection rules that facilitate decay.

The log HF calculated for transitions from the ground state to various excited states are illustrated in Fig. 5.

Further, we evaluated the standard deviation (σ) of the logarithmic half-life using the following formula:

$$\sigma = \sqrt{\frac{1}{(n-1)} \sum_{i=1}^{n} \left[\log_{10}\left(T_{1/2}^{calc.}\right)_i - \log_{10}\left(T_{1/2}^{exp.}\right)_i \right]^2}.$$

The computed standard deviation for the half-lives of nuclei undergoing transitions from the ground state to excited states in our model is 1.7671.

4. Conclusions

This manuscript presents a comprehensive investigation into the fine structure of alpha decay in odd-odd and odd-even isotopes of Americium, Berkelium, Einsteinium, and Mendelevium nuclei. We employed the CYEM, incorporating higher-order deformation parameters, spin-parity effects, and rotational energy contributions. The calculated partial half-lives for alpha transitions to excited states showed good agreement with experimental data, generally within two to three orders of magnitude. A linear relationship between the branching ratio and decay width was observed, indicating direct proportionality and suggesting consistent nuclear effects influencing the decay processes across these isotopes. This finding enhances our understanding of decay dynamics, quantum states, and the underlying nuclear structure. Additionally, the average log HF show that alpha decay is more hindered in odd-even nuclei (log HF = 1.866) compared to odd-odd nuclei (log HF = 0.961). This implies that pairing effects and spin-parity matching significantly impact decay probabilities. Interestingly, despite their complex configurations, odd-odd nuclei may exhibit more favorable decay pathways due to specific structural compatibilities or selection rules. In conclusion, the CYEM proves to be a reliable tool for analyzing the alpha decay fine structure in odd-odd and odd-even nuclei, offering valuable insights into nuclear behaviour and structure.

REFERENCES

1. C. Xu, Z. Ren. Branching ratios of α-decay to excited states of even-even nuclei. Nucl. Phys. A 778 (2006) 1.
2. Z. Ren, D. Ni. Systematics of fine structure in the α decay of deformed odd-mass nuclei. J. Phys.: Conf. Ser. 569 (2014) 012039.
3. K.P. Santhosh, J.G. Joseph, B. Priyanka. Fine structure in the α-decay of odd-even nuclei. Nucl. Phys. A 877 (2012) 1.
4. D. Ni, Z. Ren. Systematic calculation of fine structure in the α decay of deformed nuclei. J. Phys.: Conf. Ser. 381 (2012) 012055.
5. D.S. Delion, A. Dumitrescu. Systematics of the α-decay fine structure in even-even nuclei. At. Data Nucl. Data Tables 101 (2015) 1.
6. V.Yu. Denisov, A.A. Khudenko. α-Decay half-lives, α-capture, and α-nucleus potential. At. Data Nucl. Data Tables 95 (2009) 815.
7. M. Mirea. Fine structure of alpha decay from the time-dependent pairing equations. Eur. Phys. J. A 56 (2020) 151.
8. D. Bucurescu, N.V. Zamfir. Fine structure of alpha decay of even-even trans-lead nuclei – an intriguing nuclear structure paradigm. J. Phys.: Conf. Ser. 413 (2013) 012010.
9. Y.Z. Wang et al. Properties of α-decay to ground and excited states of heavy nuclei. Eur. Phys. J. A 44 (2010) 287.
10. V.Yu. Denisov, A.A. Khudenko. α decays to ground and excited states of heavy deformed nuclei. Phys. Rev. C 80 (2009) 034603.
11. K.P. Santhosh, J.G. Joseph. Systematic studies on α-decay fine structure of odd-odd nuclei in the region $83 \le Z \le 101$. Phys. Rev. C 86 (2012) 024613.
12. D.S. Delion et al. Coupled channels description of the α-decay fine structure. J. Phys. G 45 (2018) 053001.
13. K.P. Santhosh, S. Sahadevan, J.G. Joseph. Alpha decay of even-even nuclei in the region $78 \le Z \le 102$ to the ground state and excited states of daughter nuclei. Nucl. Phys. A 850 (2011) 34.
14. K.P. Santhosh et al. Systematic study on the α-decay fine structure of even-odd nuclei in the range $84 \le Z \le 102$. J. Phys. G 38 (2011) 075101.
15. G.M.C.V. Bai, R.N. Agnes. Theoretical studies on the fine structure of α decay for even-odd and even-even isotopes of Cm, Cf, Fm and No nuclei. Pramana 93 (2019) 39.
16. D. Lunney, J.M. Pearson, C. Thibault. Recent trends in the determination of nuclear masses. Rev. Mod. Phys. 75 (2003) 1021.
17. N.P. Saeed Abdulla et al. Investigation of two-proton decay using modified formation probability. Nucl. Phys. At. Energy 25 (2024) 105.
18. H.J. Krappe, J.R. Nix, A.J. Sierk. Unified nuclear potential for heavy-ion elastic scattering, fusion, fission, and ground-state masses and deformations. Phys. Rev. C 20 (1979) 992.
19. H.G. de Carvalho, J.B. Martins, O.A.P. Tavares. Radioactive decay of radium and radon isotopes by ^{14}C emission. Phys. Rev. C 34 (1986) 2261.
20. M. Wang et al. The AME 2020 atomic mass evaluation (II). Tables, graphs and references. Chin. Phys. C 45 (2021) 030003.
21. P. Möller et al. Nuclear ground-state masses and deformations: FRDM(2012). At. Data Nucl. Data Tables 109-110 (2016) 1.
22. V.I. Tretyak. Spontaneous double alpha decay: First experimental limit and prospects of investigation. Nucl. Phys. At. Energy 22 (2021) 121.
23. J.R. Nix. The normal modes of oscillation of a uniformly charged drop about its saddle-point shape. Ann. Phys. 41 (1967) 52.
24. O.M. Povoroznyk, O.K. Gorpinich. Experimental observation of neutron-neutron correlations in nucleus ^{6}He from ^{3}H(α, pα)nn reaction. Nucl. Phys. At. Energy 20 (2019) 357.
25. P. Möller, J.R. Nix, W.J. Swiatecki. Calculated fission properties of the heaviest elements. Nucl. Phys. A 469 (1987) 1.
26. D.N. Poenaru et al. Heavy cluster decay of trans-zirconium “stable” nuclides. Phys. Rev. C 32 (1985) 2198.
27. X.D. Sun et al. Systematic study of α decay half-lives of doubly odd nuclei within the two-potential approach. Phys. Rev. C 95 (2017) 044303.

Р. Нітія Агнес[1,*], Г. М. С. В. Бай[2], С. Селвакумар[3], С. К. Велла Дурай[4]

[1] Фізичний факультет, Коледж Святого Джона, Палаямкоттай, Тамілнад, афілійований до Університету Манонманіама Сундарнара, Тірунелвелі, Тамілнад, Індія
[2] Фізичний факультет, Державний гуманітарний коледж, Нагеркойл, Тамілнад, афілійований до Університету Манонманіама Сундарнара, Тірунелвелі, Тамілнад, Індія
[3] Фізичний факультет, Відділення природничих і гуманітарних наук, Інженерний коледж Тамірабхарані, Татчаналлуру, Тірунелвелі, Тамілнад, Індія
[4] Магістратура та науково-дослідницький фізичний факультет, Коледж Шрі Парамакалаяні, Алваркурічі, Тенкасі, Тамілнад, Індія

*Відповідальний автор: nithya.phy@stjohnscollege.edu.in

КОМПЛЕКСНЕ ДОСЛІДЖЕННЯ ТОНКОЇ СТРУКТУРИ АЛЬФА-РОЗПАДУ В НЕПАРНО-НЕПАРНИХ ТА НЕПАРНО-ПАРНИХ ЯДРАХ

Проведене комплексне дослідження тонкої структури альфа-розпаду в непарно-парних і непарно-непарних ядрах з атомними номерами 95 - 101. Використовуючи кубічну плюс Юкава плюс експоненціальну модель,

розглянуто комбіновані ефекти Кулонівського потенціалу, відцентрового потенціалу і Юкава плюс експоненціального потенціалу як бар'єра для взаємодіючих фрагментів, з доповненням кубічним потенціалом в області перекриття. Наші розрахунки парціальних періодів напіврозпаду для альфа-переходів на збуджені стани продемонстрували гарне узгодження з експериментальними даними, даючи стандартне відхилення 1,7671 для логарифмів періодів напіврозпаду. Крім того, аналіз тонкої структури виявив лінійну кореляцію між імовірністю заселення та шириною розпаду в альфа-розпадах для таких ядер, як америцій, берклій, ейнштейній і менделевій, що вказує на пряму пропорційність між цими параметрами.

Ключові слова: альфа-розпад, тонка структура, енергія розпаду, ядра, Юкава плюс потенціал.

Надійшла / Received 14.04.2025